Journal of the Electrochemical Society, Vol. 141, No.1, 1994, pp.83-90.
Print ISSN: 0013-4651
Online ISSN: 1945-7111
DOI: 10.1149/1.2054714
http://scitation.aip.org/JES
http://scitation.aip.org/getpdf/servlet/GetPDFServlet?filetype=pdf&id=JESOAN000141000001000083000001&idtype=cvips&prog=normal

X-Ray Absorption Study of Electrochemically Grown Oxide Films on AlCr Sputtered Alloys II. *In Situ* Studies

G. S. Frankel,*[,a] A. G. Schrott,[a] A. J. Davenport,*[,b] H. S. Isaacs,*[,b] C. V. Jahnes,[a] and M. A. Russak[a]

[a]IBM Research Division, T. J. Watson Research Center, Yorktown Heights, New York [b]Department of Applied Science, Brookhaven National Laboratory, Upton, New York
* Electrochemical Society Active Member.

ABSTRACT

The chemistry of chromium in the passive film on sputter-deposited chromium and AlCr thin films has been investigated *in situ* in an electrochemical cell under potential control by studying x-ray absorption near edge structure. At high potentials, Cr in the AlCr alloys was oxidized to the 6-valent state. Depending on the rate of potential increase, 6-valent chromium either dissolved from the alloy or was trapped in the passive film where it was electroactive, *i.e.*, the valence state could be reversibly switched between the 3- and 6-valent states by changing the applied potential. The kinetics of these processes were investigated. *Ex situ* x-ray photoelectron spectroscopy measurements indicated that, during slow scanning at low potentials, the composition of both the surface oxide and underlying metallic layers changed. These changes resulted in a structure that was susceptible to transpassive dissolution of Cr at potentials above 0.2 V(MSE).

The chemistry of chromium in passive oxide films is of interest due to the corrosion resistance it imparts as an alloying element. The valence state is conventionally studied using techniques such as Auger electron spectroscopy (AES) and x-ray photoelectron spectroscopy (XPS). However, these techniques detect emitted electrons, and measurements can only be carried out post-exposure in a vacuum. X-ray absorption spectroscopy (XAS) has recently been applied to the study of chromium in oxide films on metals.[1-10] The detailed structure of the edge (x-ray absorption near edge structure, XANES) is particularly sensitive to the presence of 6-valent chromium due to the appearance of a sharp peak just below the edge. Furthermore, as XAS only uses x-rays, *in situ* measurements can be carried out in an aqueous solution while the sample is under potential control.[6-10]

The chemistry of chromium in oxide films on aluminum treated in chromate solution has been studied using XANES by a number of authors.[1-4] Hawkins *et al.*[1] found both 3- and 6-valent chromium in oxide films produced by anodization of aluminum in a borate buffer and subsequent exposure to a chromate solution at open circuit. The thinner the oxide film, the greater was the proportion of 3-valent chromium. Chung *et al.*[2,3] investigated the chemistry of chromium in oxide films formed by anodizing aluminum in a chromate solution. They also found both 3- and

6-valent chromium with the 6-valent chromium predominantly on the outside of the film. Wainright *et al.* [4] studied the sealing in dichromate solution of aluminum which had previously been anodized in sulfuric acid. The chromium co-ordination in the oxide film most closely resembled that of a chromate standard.

In the present study, XANES was used to study chromium in the passive oxide film on AlCr alloys. Thus chromium was introduced into the film from the metal rather than from the solution side of the interface. Previous *ex situ* glancing incident angle XANES experiments on polarized AlCr alloys[5] have shown that, at and above 0.7 V (MSE) in pH 7.4 boric-borate solution, both 3- and 6-valent chromium were in the passive film, with the 6-valent chromium increasingly observed at higher potentials and predominantly in the outer part of the film.

We have recently demonstrated the feasibility of measuring the valence state of chromium *in situ* during electrochemical polarization using XANES.[6] In the present paper, we describe the effect of the rate of potential increase on the behavior of chromium in the passive oxide film on AlCr alloys. Measurements were made while the samples were exposed to bulk solution and under electrochemical control.

Experimental

The cell design (which has been described previously[6]) was based on that used by Kerkar *et al.*[7] for extended x-ray absorption fine structure (EXAFS) measurements. The working electrode was a thin metal film deposited on a thin plastic sheet, which became the window of a 50 ml electrochemical cell. The incident x-ray beam and resulting fluorescent x-rays passed through the thin plastic. An area of 1.7 cm^2 of metal was in contact with bulk solution (0.5*M* H_3BO_3 + 0.05*M* $Na_2B_4O_7$ with pH 7.4), which was exposed to laboratory air. The cell also contained a mercurous sulfate reference electrode (MSE, 0.64 V (SHE)) and a platinum wire counterelectrode. All potentials are quoted with respect to the MSE scale.

The samples were pure chromium and AlCr alloys in the form of sputtered films of 20 and 40 Å thickness. Thin films were used so that most or all of the alloy was oxidized when the passive layer was formed, thereby minimizing the signal from metallic chromium in the underlying alloy. The films were deposited on thin Mylar sheets (~6 μm) which were first sputter-coated with 100 Å of Ta or Nb for electrical contact. Ta underlayers were used for XAS measurements. For XPS, however, Nb underlayers were used in order to avoid the overlap of the Cr 3p line and the plasmon loss peak associated with the Ta 4f line. No difference between the behavior of films deposited on Nb and Ta was observed. The thin films were dc magnetron sputtter-de-posited in 5 mTorr Ar after first pumping the chamber to a pressure of 3×10^{-7} Torr. The AlCr alloys were deposited on the metallic underlayers without breaking vacuum. Mosaic targets composed of Al and Cr segments were used to ensure compositional uniformity.

XAS measurements were made on Beamline X19A at the National Synchrotron Light Source at Brookhaven National Laboratory. The electrode was placed at a 45° angle to the incident monochromatic x-rays. Measurements were made at the Cr K edge using a Cowan fixed exit-height double-crystal monochromator with a resolution of better than 2 eV (determined from the width of the Cr(VI) pre-edge peak at 5993 eV). The monochromator was calibrated by setting the energy of the maximum slope in the first part of the Cr metal K edge to be 5989 eV. Fluorescent Cr Kα radiation was detected through the back of the electrode with a 13-element solid-state detector (Canberra) placed at 90° to the incident x-rays. Such an energy-discriminating detector is required in order to detect the small chromium fluorescence signal against the high background of incident radiation scattered by the cell and solution. Dead-time

problems were avoided by ensuring that the total count rate in each detector element never exceeded 30,000 counts/s. The beam size was approximately 1 mm × 10 mm and the beam was left in the same position on the cell throughout each experiment. The background signal was subtracted out of each spectrum by fitting a curve to the signal below the edge. Since the beam size was controllable and reproducible, changes in the edge height reflect changes in the total quantity of Cr in the samples.

Most spectra were collected by scanning the incident beam energy from 5970 to 6040 eV with coarse energy steps (typically 2 eV) and short counting time per step (2 to 3 s) in order to minimize the total collection time. Smaller energy steps (0.5 eV) were used around the pre-edge peak in order to determine whether any 6-valent chromium was present, and larger energy steps (5 eV) were used in the range above the edge. These fast spectra took about 3 min to complete, which enabled time-dependent changes to be monitored. Higher quality spectra were occasionally obtained by using small energy steps and increased counting time.

The XPS measurements were made in a VG ESCALAB MK II with a 150° hemispherical analyzer using a 20 eV pass energy and non-monochromatized Al Kα radiation. The source satellites were numerically subtracted out. The samples were prepared in a manner identical to that used in the XAS experiments, and then introduced in the vacuum chamber within minutes after polarization. The oxide films exhibited charging during XPS measurement, as evidenced by the energy position of the C 1s line, which arises from adventitious carbon. Because C was at the same potential as the insulating oxide, whereas the metal was directly connected to the spectrometer, the position of the C 1s peak and the energy separation of the Al(0) and Al(III). peaks varied depending on the extent of charging. Unlike the previous *ex situ* work in which the energy of the C line and thus the Al(III) line were fixed,[5] in this work the spectra were not shifted in position to account for charging. Using this approach, the metallic peaks are aligned and the positions of the oxide peaks shift to higher binding energy as a result of the effects of surface charging. This approach better reflects the physical situation.

Results

The behavior of a 20 Å thick, Al-12%Cr alloy upon stepping the potential from open circuit to +2 V was described previously,[6] and the data are reproduced in Fig. 1. Cr(VI) was found in the passive film formed at 2 V. This chromium was electroactive and could be reduced to the 3-valent state by stepping the potential to -1.5 V.[6] Edges of standard compounds characteristic of the different valence states of chromium are shown as broken lines in Fig. 1 along with the experimental data from AlCr alloys, which are shown as solid lines. Chromium metal (edge a) has the lowest absorption edge energy. The spectrum for the alloy at open circuit (-1.0 V for this sample) directly overlies the Cr metal edge, indicating that Cr is only present in the metallic state and the surface oxide film is purely alumina. While it is difficult with XAS to see a small amount of Cr(III) in the presence of a dominant quantity of chromium metal (see below), this result is consistent with XPS measurements of as-deposited alloy films containing less than about 30% Cr.[5]

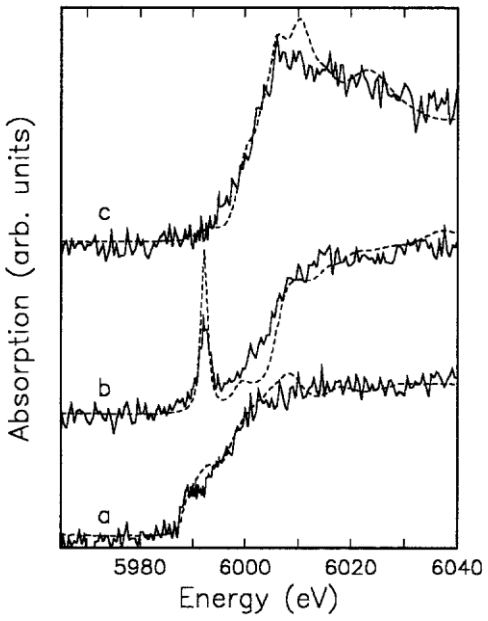

Fig. 1. ***In situ*** **XANES measurement of the Cr K edge of a 20 Å Al-12%Cr film in a borate buffer solution: a, at open circuit; b, after 7 min at 2 V (MSE); c, after 6 min at -1.5 V (MSE) (solid lines). The broken lines show standard compounds measured in transmission: a, Cr; b, K_2CrO_4; and c, Cr_2O_3.[6]**

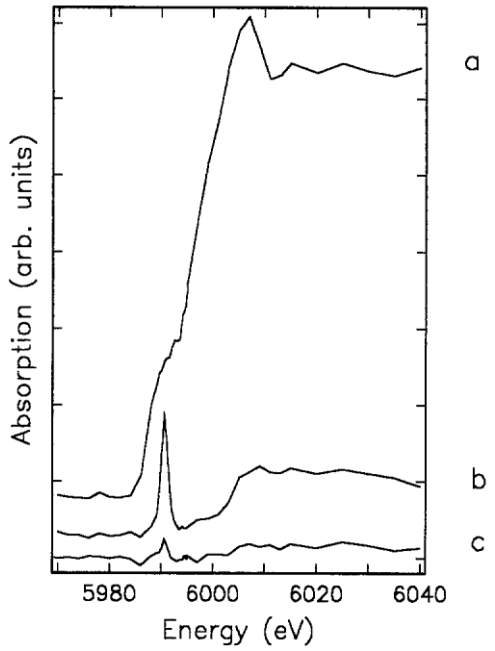

Fig. 2. Cr K edge for a 40 Å film of pure chromium; a, at open circuit, and b, 0 to 3 min and c, 3 to 6 min after stepping the potential to +1.5 V (MSE).

The standard in curve b of Fig. 1 is for 6-valent chromium (K_2CrO_4), which has an edge at a higher energy than chromium metal and a very sharp pre-edge peak at 5993 eV. This pre-edge peak is associated with the tetrahedral coordination found for 6-valent chromium compounds[11] and is a very useful fingerprint for the presence of Cr(VI). It can be seen even in the presence of a substantial amount of chromium in other valence states, which contribute little or no signal at this energy. This peak can also provide semiquantitative information on the amount of Cr(VI) present; the ratio of the pre-edge peak height to the edge height approximately equals the ratio of Cr(VI) to the total chromium present.[10] In this fashion, the Cr in the sample held at 2 V can be seen to be about half 6-valent, the other half being in the 3-valent state.

The standard in curve c of Fig. 1 is for 3-valent chromium (Cr_2O_3). The edge position is midway between those of Cr(0) and Cr(VI), no sharp pre-edge peak is present, and a broad peak is present directly at the top of the edge. The data for the AlCr sample polarized at −1.5 V almost directly overlie the Cr_2O_3 standard, and little change in edge height is seen compared to the spectra taken at the other two potentials. (Note that the data from the AlCr alloys were not normalized, whereas the spectra of the standards were normalized to the edge heights of the AlCr alloy spectra.) This indicates that the Cr present in the 6-valent state at 2 V was reduced to Cr(III) during polarization at −1.5 V with little dissolution.

Figure 2 shows an experiment similar to that in Fig. 1, but using a 40 Å pure chromium sputtered layer. The x-ray absorption edge measured at the open-circuit potential, −0.58 V, is given in curve a of Fig. 2. This spectrum has the characteristics of the chromium metal spectrum (see curve a of Fig. 1). The passive oxide film, presumably 3-valent chromium, was thin and not discernable in the spectrum dominated by the signal from the underlying 40 Å of metallic chromium at lower energy. One limitation of XANES is that the signal from a small proportion of a higher valence state having a higher binding energy would only cause a small perturbation of the absorption edge of the dominant lower-valent-state species. The exception to this is Cr(VI) because its pre-edge peak is an extremely sharp feature that appears below the Cr(III) edge and only halfway up the Cr(0) edge. Thus, one or two monolayers of chromium oxide would not be detectable on 40 Å of metallic Cr using XAS.

When the potential was stepped to +1.5 V, a rapid 3-min spectrum was initiated, curve b of Fig. 2. By the time the energy had reached the edge position (~1 min), some of the chromium was present in the 6-valent state, as indicated by the pre-edge peak (see curve b of Fig. 1). Furthermore, the large decrease in edge height indicates that a substantial proportion of the chromium had dissolved by the end of the spectrum collection. The observation that the pre-edge peak is higher than the edge in curve b of Fig. 2 (which is not the case for 6-valent chromium standard compounds) is due to the fact that the chromium was continuously and rapidly dissolving, so more was present in the middle of the spectrum than at the end. By the time a second spectrum was completed 6 min after the potential step, little chromium was detectable above the background noise.

The critical potential for the onset of transpassive dissolution of a 20 Å pure chromium film was determined by stepping the potential in 100-mV steps from the open-circuit potential and initiating a rapid (3-min) spectrum at the beginning of each potential step. The results are shown in Fig. 3, where it can be seen that the K edge remained predominantly metallic from open circuit to +0.1 V. At +0.2 V, the 6-valent chromium pre-edge peak emerged and loss of chromium via dissolution is apparent from the decrease in the height of the edge. The edge measured at 0.3 V indicates that only a fraction of the original Cr content remained. The critical potential for formation of, chromate, 0.2 V, is higher than the theoretical equilibrium potential

calculated by Pourbaix, which ranges from −0.24 to −0.1 V depending on the Cr(III) species used in the calculation.[12]

The previous experiment was repeated for AlCr alloys with a number of different chromium concentrations. Figure 4 shows data for an alloy that was 20 Å thick and contained 22% chromium. The potential was stepped from open circuit to −0.7 V and then increased in incremental steps of 100 mV until reaching +0.7 V. At each potential, a rapid edge spectrum was obtained and the current was measured. Selected spectra are shown in Fig. 4 where they are labelled with the potential maintained during collection of the spectrum. At the open-circuit potential, the chromium was in the metallic state, and the spectra from −0.7 to −0.3 V also indicated metallic chromium. Around −0.2 V there was a transition to 3-valent chromium which persisted until 0.1 V. At +0.2 V, a very small pre-edge peak characteristic of 6-valent Cr appeared and dissolution was significant, as is apparent from the lower edge height. Cr continued to dissolve until 0.4 V. Selected current transients are shown in Fig. 5 and the current densities measured at the end of each spectrum are shown in Fig. 6. The current reached a maximum at 0.2 V, coinciding with the appearance of Cr(VI) and significant dissolution. The current decreased above 0.2 V as the Cr in the film was depleted.

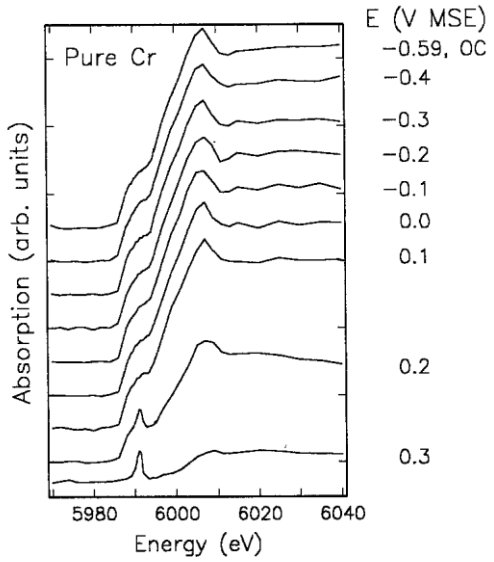

Fig. 3. Cr K edge for a 40 Å film of pure chromium at open circuit and during stepwise anodic polarization in a borate buffer. The potential was incremented to the potential indicated at the beginning of each 3-min energy spectrum.

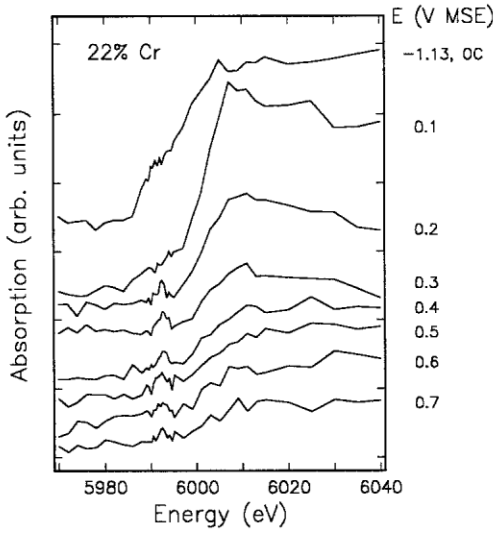

Fig. 4. Cr K edge for a 20 Å Al-22%Cr alloy polarized in a borate buffer solution at the potentials indicated. The potential sequence is described in the text. Each spectrum took about 3 min to collect.

Similar experiments using incrementally increased potential were performed on Al-12%Cr (Fig. 7), Al-43%Cr (not shown), and Al-53%Cr (Fig. 8). In all cases, Cr(VI) was not observed until the critical potential of 0.2 V. For the 53%Cr sample, some underlying metallic Cr could be seen up to 0.3 V, as evidenced by the shoulder near 5990 eV.

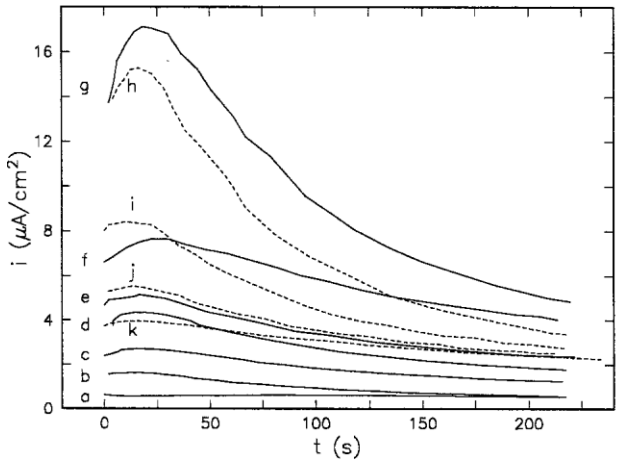

Fig. 5. Current transients measured for the sample shown in Fig. 4 at the following potentials in V: a, −0.7; b, −0.5; c, −0.3; d, −0.1; e, 0; f, 0.1; g, 0.2; h, 0.3; i, 0.4; j, 0.5; k, 0.7. Curves a-g are solid and h-k are dashed lines.

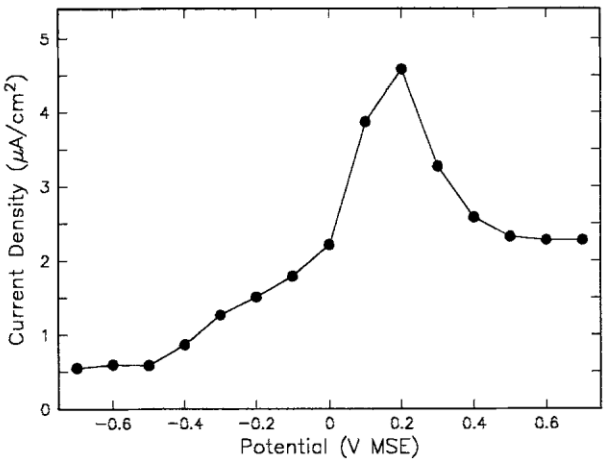

Fig. 6. Current densities at the end of each potential step for the sample shown in Fig. 4.

Figure 9 shows the charge associated with each potential step (partial charge) and the cumulative charges for the samples with different Cr content. The cumulative charge at 0.1 V for all cases was less than the expected charge for trivalent oxidation of all Cr and Al atoms in the 20 Å thick films (6 to 7.5 mC/cm^2, depending on Cr content). The increase in charge starting at 0.2 V results partially from oxidation of Cr(III) to Cr(VI). A larger charge is passed for the 53%Cr sample in the range of 0.2 to 0.4 V because of the larger quantity of Cr. However, the charges passed at potentials above 0.2 V are much larger than those expected for the further oxidation of Cr(III) alone (1 to 4 mC/cm^2). As will be described below, the XPS data show that Nb starts to oxidize at this point and this oxidation adds to the charge. There is also the possibility that some oxygen evolution may take place at the higher potentials. The ampero-metric data are complicated by these side reactions.

It is evident, from a comparison of Fig. 1 and 7, that during slow polarization of AlCr alloys through +0.2 V chromium can dissolve via formation of chromate, whereas if the potential is stepped directly to a high value (+2 V), the chromate is trapped in the film and does not dissolve into solution. The question then arises as to whether trapping 6-valent chromium in the passive film at high potential will prevent its dissolution if the potential is subsequently raised slowly through the critical potential of 0.2 V. The results of this experiment, carried out on a 40 Å Al-12%Cr alloy, are shown in Fig. 10. The first edge (top of Fig. 10) was taken 20 min after the potential was stepped to 2 V. The pre-edge peak indicates the presence of some 6-valent

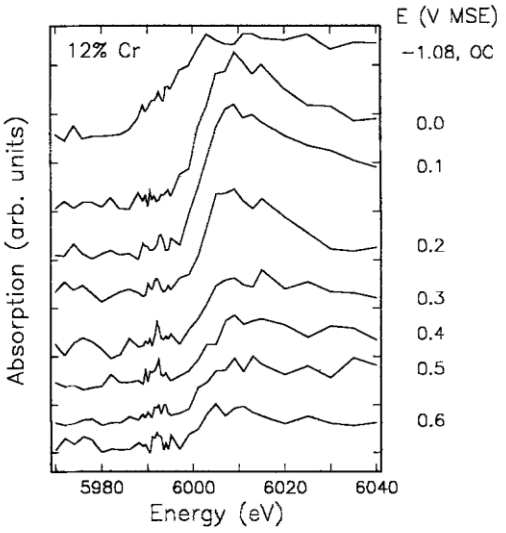

Fig. *7.* Cr K edge for Al-12%Cr (20 Å) at the potentials shown during stepwise polarization from open circuit.

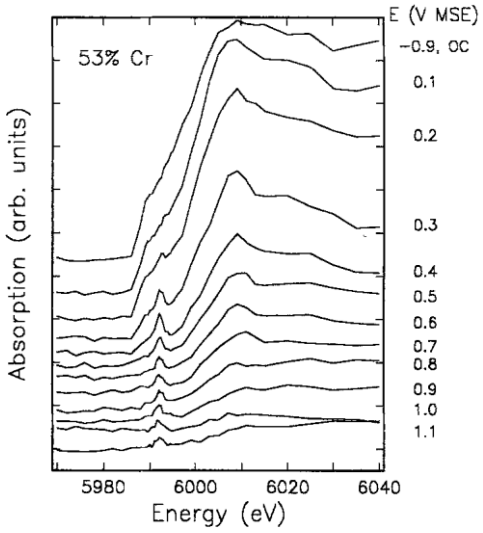

Fig. 8. Cr K edge for Al-53%Cr (20 Å) at the potentials shown during stepwise polarization from open circuit.

chromium in the film, which was then reduced to the 3-valent state by stepping the potential down to −1.5 V (second edge). The potential was then stepped to −0.5 V and increased by 100 mV at 3-min intervals during which edges were measured. At +0.7 V, the x-ray beam went down, and the potential was maintained at the value for 2 h until data collection could resume. From +0.8 V, the potential was increased in 200-mV steps up to 2 V. As the potential was increased through 0.2 V, the critical value for dissolution, no 6-valent chromium peak was apparent and the edge height remained constant so no dissolution was taking place. The pre-edge peak only appeared after the sample was held at +0.7 V for 2 h. Even after re-emergence of the

pre-edge peak, the edge height was unchanged from earlier measurements, so no significant dissolution was taking place.

Because edges can be measured relatively rapidly (in about 3 min), it is possible to study the kinetics of processes that take place over a sufficiently long period. Figures 11 to 14 show a sequence of measurements on a 40 Å thick sample of Al-12Cr that demonstrates this. The potential of a fresh sample was stepped from open circuit (with chromium in the metallic state, top edge in Fig. 11) to 2 V. Starting simultaneously with the potential step, a series of three fast edges was collected. The first of these shows that the chromium was immediately oxidized to the

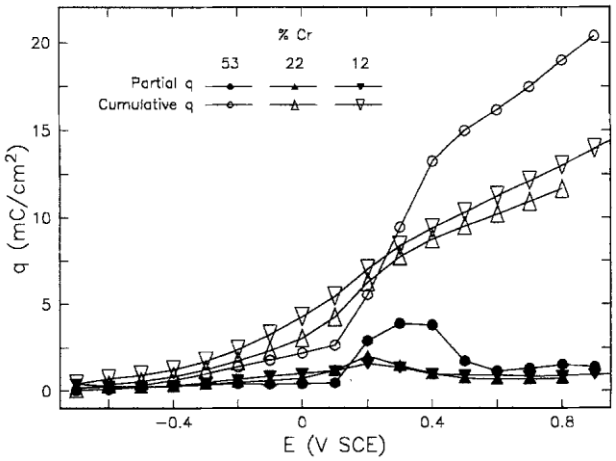

Fig. 9. Charge passed for the samples shown in Fig. 4, 7, and 8. Partial charges reflect the charge passed during each potential step, and cumulative charges are sums of the charge passed at all lower potentials.

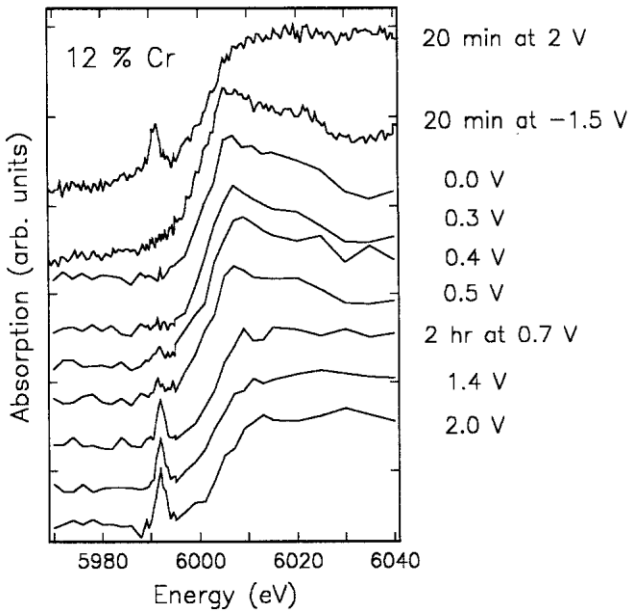

Fig. 10. Cr K edge for a 40 Å Al-12%Cr alloy which has been polarized at +2 V (MSE), then polarized at -1.5 V (MSE) and then stepped at 100-mV intervals from -0.5 V (MSE) to +0.7 V (MSE) where the potential was maintained for 2 h and then stepped in 200-mV intervals from +0.8 V (MSE) to 2 V (MSE). Edges are shown for selected potentials.

3-valent state. A small and rather noisy shoulder at the beginning of the edge may indicate that there was still some remaining metallic chromium. However, none of edges show any sign of 6-valent chromium. The characteristic pre-edge peak only appeared during a more detailed spectrum which was initiated 9 min after the original potential step and took 32 min to complete. The height of the pre-edge peak (and thus the proportion of 6-valent chromium) continued to increase and was significantly higher in another detailed spectrum which was collected between 50 and 77 min after the potential step, exhibiting a final Cr(VI) content of about 55%.

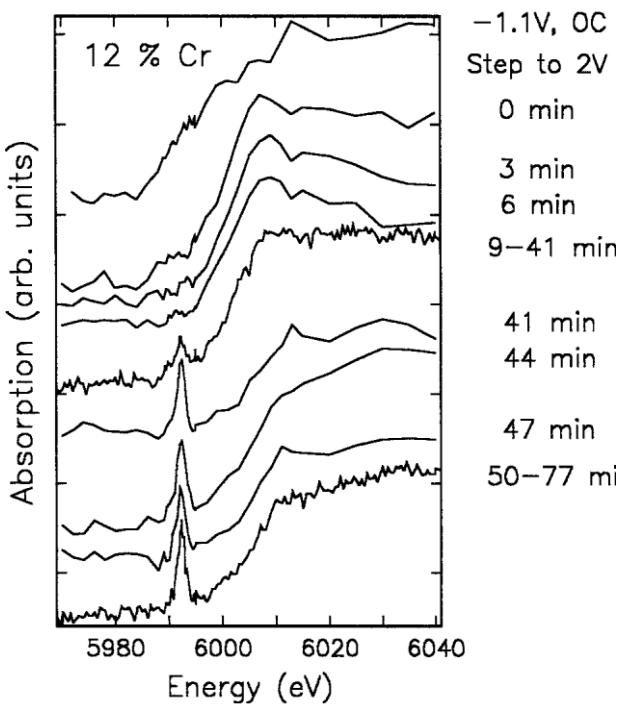

Fig. 11. Cr K edge for 40 Å of Al-l2%Cr alloy. The potential was stepped from open circuit to 2 V (MSE) and edges were collected at the times indicated.

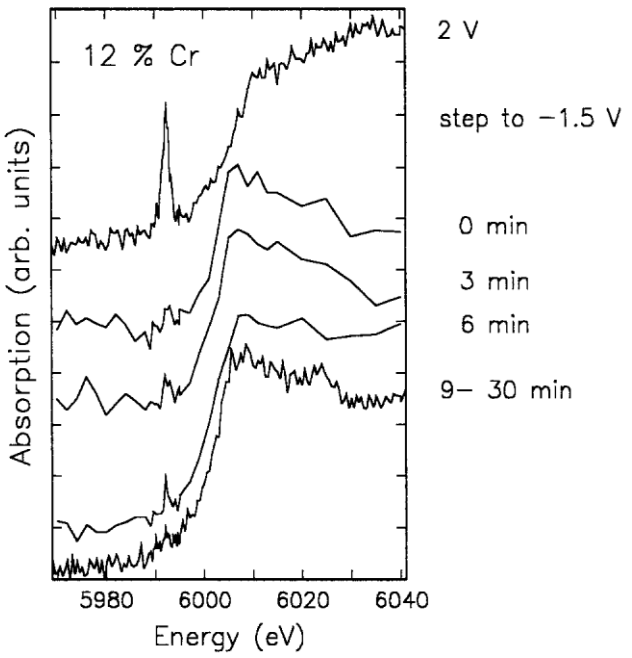

Fig. 12. Continuation of the experiment shown in Fig. 11. The last edge of Fig. 11 has been replotted as the first of Fig. 12. The potential was stepped from +2 V (MSE) to -1.5 V (MSE) and edges were collected at the times indicated.

Additional experiments (not shown) indicate that the kinetics of the Cr(III) to Cr(VI) oxidation depended on both potential and Cr content. A 12% Cr sample polarized to 0.7 V did not start to form Cr(VI) after 44 min, whereas a 22% Cr sample polarized to 0.7 V exhibited about 20% Cr(VI) after 1 h.

The last edge in Fig. 11 is reproduced at the top of Fig. 12. After this edge was collected, the potential was stepped down to −1.5 V and another series of three fast spectra was collected. These all show a 3-valent edge with perhaps a very small and noisy pre-edge peak indicating some small amount of residual 6-valent chromium. No pre-edge peak was present in the slower, detailed spectrum which was subsequently taken (bottom edge in Fig. 11). This indicates that the reduction of 6 to 3-valent chromium was more rapid than the initial oxidation process and very little Cr was lost in the oxidation/reduction cycle.

The last edge in Fig. 12 is reproduced at the top of Fig. 13. The 3-valent chromium was then oxidized to the 6-valent state by stepping the potential back to +2 V. The three fast spectra collected immediately after the potential step show a small and increasing pre-edge peak. Comparison of Fig. 11 and 13 indicates that the second oxidation process took place more rapidly than the first one.

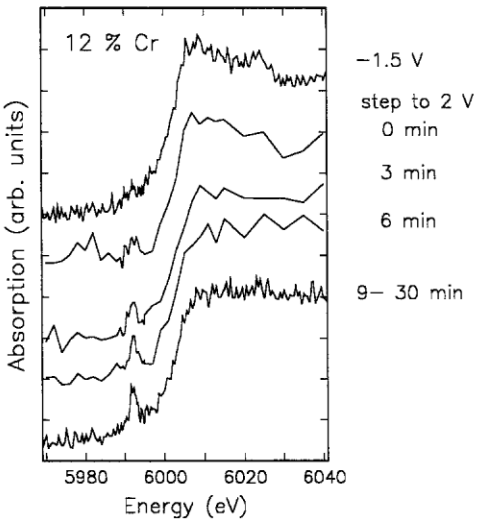

Fig. 13. Continuation of the experiment shown in Fig. 11 and 12. The last edge of Fig. 12 has been replotted as the first of Fig. 13. The potential was stepped from -1.5 V (MSE) to +2 V (MSE) and edges were collected at the times indicated.

The last edge in Fig. 13 is reproduced at the top of Fig. 14. The potential was stepped from +2 V down to −1.6 V in 200-mV intervals. The pre-edge peak only began to disappear at -1.4 V indicating that low applied potentials were required for the reduction process to occur.

In order to understand better the behavior of Cr in the AlCr alloys, XPS analysis was performed on a number of samples. XPS previously was used to investigate the presence of Cr(VI) and determine the Cr:Al ratio in the oxides formed on samples exposed at high potentials.[5] In this work, XPS was used to focus on the state of Al and Cr after exposure at lower potentials.

Figure 15 shows *ex situ* XPS data collected from a set of 25 Å Al-22%Cr samples deposited on Mylar with a 100 Å interlayer of Nb. The curves are normalized to the background at 85 eV. Curve a was collected from an "as received" freshly deposited sample. The sample was introduced into the spectrometer immediately after deposition and was thus exposed to air for only 5 min. Four features are apparent. A doublet of Al 2p peaks is seen at 72 and 75 eV, representing metallic Al(0) and Al(III), respectively. The stronger Al(III) signal results from the air-formed film on the surface of the sample. The relative areas of the two peaks do not directly represent the volume fraction of the two species as the signal from the underlying metal is attenuated by the surface oxide. The broad feature at 56 eV is the signal from the Nb 4s line arising from the Nb under-layer. The energy position corresponds to metallic Nb, indicating that the alloy layer was continuous over the under-layer and did not form isolated islands. At 41 eV is the Cr 3p peak. The position of this peak indicates that the Cr was also entirely metallic. As found previously,[5] Al is selectively oxidized on exposure to air because of its high reactivity relative to Cr, forming a protective alumina film.

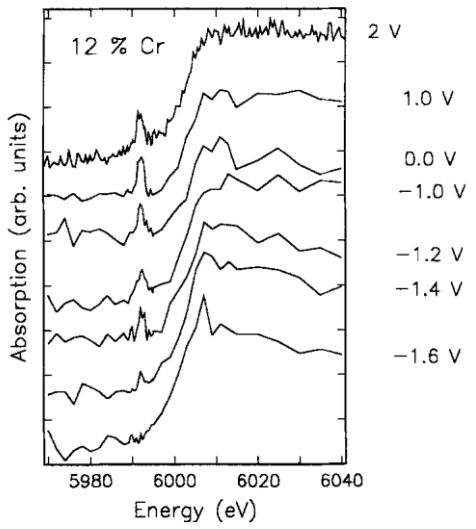

Fig. 14. Continuation of the experiment shown in Fig. 11 to 13. The last edge of Fig. 13 has been replotted as the first of Fig. 14. The potential was stepped from +2 V (MSE) down to −1.6 V (MSE) in 200-mV intervals.

The XPS spectrum after potentiodynamically polarizing a sample at 0.5 mV/s [a rate close to the nominal rate of increase during slow potential stepping in the XAS experiments (0.1 V every 3 min)] from open circuit to +0.5 V is shown in curve b of Fig. 15. This sample was thus prepared similarly to the one from which the XAS edge shown in Fig. 4 at 0.5 was obtained. The XPS results show that both Al and Cr were present only in the +3 valence state with much reduced peak areas. Note that the feature at 50 eV is associated with the Nb signal and is not indicative of Cr(VI). The smaller Al and Cr peaks, along with the increased signal from Nb, suggest that Al and Cr have dissolved to some extent during the polarization treatment. Most of the Nb signal derived from oxidized Nb (probably Nb^{+5}). For all of the samples examined, oxidation of Nb occurred only after complete oxidation of the AlCr film. This was either because the AlCr film lost integrity or because complete oxidation of the overlying AlCr film allowed the electric field to penetrate to the Nb underlayer and oxidize some of the Nb. Angle-resolved XPS data suggest that the oxidized Nb was in fact exposed at the surface.

The binding energy of the Al(III) peak for all of the alloy samples that were subjected to anodic polarization (curves b to e in Fig. 15) is somewhat lower than the energy for the Al (III) species in the as-received sample. This shift has been attributed to a lesser extent of charging as a result of the formation of a more conductive, Cr-containing, surface oxide film, compared to the ambient-formed oxide that is only aluminum oxide.[5] The oxides on pure Al in the as-received state or after polarization have a 3p peak with the same energy as that observed for the air-formed oxide on the AlCr alloys. Because the C 1s line is at the same energy for these three cases, the extent of charging is similar and larger than for the conductive oxide formed on polarized AlCr alloys. If the spectra are corrected for charging, the Al(III) peaks for all samples fall at the same energy.

In sharp contrast to the results of the potentiodynamic experiment are the results shown in curve c of Fig. 15, which were obtained by stepping the potential from open circuit directly to +0.5 V and maintaining it there for 1000 s. A very strong Al(III) signal was present with a

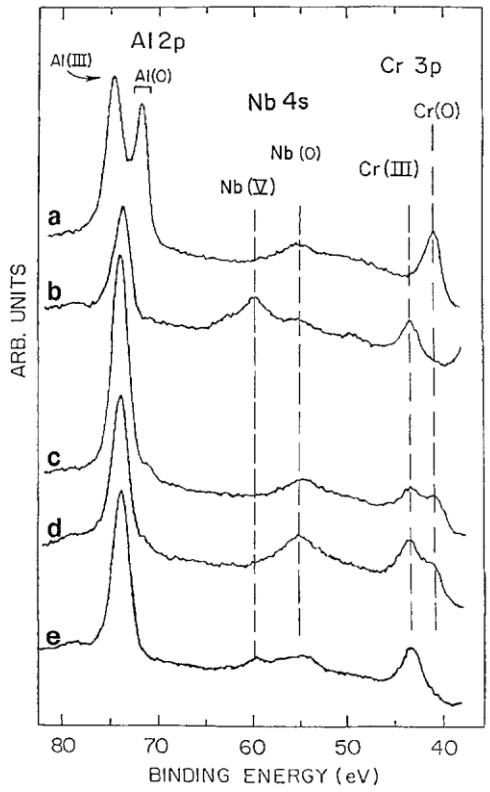

Fig. 15. XPS spectra for 25 Å thick Al-22%Cr films on Mylar coated with 100 Å of Nb: a, as received; b, after potentiodynamic polarization to 0.5 V (MSE); c, after potentiostatic polarization at 0.5 V; d, after potentiodynamic polarization to 0 V; e, after potentiodynamic polarization to 0 V followed by stepping the potential to 0.5 V. The spectra are normalized to the background signal at 85 eV.

small metallic shoulder at lower binding energies. Nb remained entirely in the metallic state, indicating that the AlCr film was still continuous. The chromium was present in both +3 and metallic states. No 6-valent Cr was observed; it should be noted that the potential of +0.5 V is considerably below 2 V, that used in Fig. 1, 10, 11, and 13 where 6-valent Cr formed within minutes. As mentioned, it take much longer at 0.7 V than at 2 V to form 6-valent Cr.

The changes that take place below the critical potential for transpassive Cr dissolution, 0.2 V, were investigated by potentiodynamically polarizing a sample from open circuit again at 0.5 mV/s, but stopping the potential at 0 V. Curve d in Fig. 15 indicates that a significant change took place below the transpassive potential. Similar to curve b, the total Al peak area was much smaller than that observed for the as-received condition. Aluminum was present almost entirely in the oxidized state with only a very slight shoulder indicating some residual metallic Al. Cr was present in a mixture of +3 and metallic states. Both the peak area in this spectrum and the *in situ* XANES measurements (Fig. 4) indicate that no Cr had dissolved. The Nb signal was stronger and entirely metallic, demonstrating that AlCr film was thinner but still continuous. Thus polarization to 0 V causes dissolution of some Al, but no Cr.

Curve e in Fig. 15 was obtained after scanning the potential to 0 V in the same manner as that used to generate curve d, and then stepping to 0.5 V and holding for 1000 s (equal to the time to scan from 0 to 0.5 V at 0.5 mV/s). The Al peak changed little after the additional

treatment, although the very small metallic shoulder was no longer present. The Cr was present only in the oxidized state, and the total Cr peak area was diminished by 20% with respect to the air-exposed initial condition, curve a. However, the real loss of Cr may be larger because the Cr signal in curve a was attenuated by the alumina surface layer. The substantial loss of Al and Cr has allowed in this case some of the Nb to be oxidized.

Discussion

Polarizing pure chromium above 0.2 V results in its rapid dissolution as chromate ions, as shown in Fig. 2 and 3. This phenomenon is independent of the rate of polarization. Polarization of AlCr alloys also causes oxidation of chromium to the 6-valent state. However, whether the Cr(VI) dissolves into the electrolyte or remains trapped in the oxide depends on the polarization sequence; stepping the potential directly to a high value (2 V) from open circuit, as in Fig. 1,10, and 11, results in trapping of 6-valent chromium in the oxide film with little dissolution, whereas progressive stepping through the critical potential of 0.2 V using 3-min long 100-mV steps or slow potentiodynamic scanning results in dissolution of chromium. The emergence of a small Cr(VI) peak in the XAS spectra when dissolution starts suggests that Cr dissolves as Cr(VI) is formed. This behavior was observed for AlCr alloys of different chromium contents ranging from 12 to 53%.

Stepping the potential directly to +2 V from open circuit causes immediate oxidation of the chromium in AlCr from the metallic state to the 3-valent state. Only after some minutes does it start to transform to the 6-valent state, the reaction being substantial after an hour. Once Cr(VI) is trapped in the oxide film by stepping the potential to 2 V, it is electroactive, *i.e.*, it can be switched between the 3- and 6-valent states by switching the potential between -1.5 V and +2 V, as shown in Fig. 1,10, and 12 through 14. Furthermore, after this initial rapid oxidation of the alloy, the chromium will then not dissolve from the oxide upon sequential reduction and reoxidation by stepping the potential through the critical potential of 0.2 V using 3-min 100 mV steps (Fig. 10).

During experiments in which there was rapid dissolution of Cr (see Fig. 2, 3, 4, 7, and 8), the XAS signal associated with Cr(VI) may derive from chromate in solution within a few tens of microns from the electrode surface, or from Cr(VI) transiently in the oxide film prior to dissolution. The fact that the Cr edge drops during the time of the experiments shows clearly that, once dissolved, the chromate diffuses away into the bulk of the solution and is no longer detected. The resulting aqueous solution has a Cr concentration that is too dilute for the sensitivity of the technique. Figure 2 indicates that, in a matter of minutes, chromate in solution will diffuse away and become undetectable. For experiments in which the potential was stepped directly to a high value, the Cr(VI) signal is stable with time, indicating that it must be trapped in the oxide film. This has been confirmed by XPS measurements of Cr(VI) in oxides on AlCr alloys stepped to high potentials.[5]

The XPS data provide an explanation for the behavior of the AlCr alloys because information on both Al and Cr is obtained. The state of the AlCr film when the potential is increased above the critical potential for transpassive dissolution seems to determine the behavior of the Cr. The exact state of the film, *i.e.*, the concentration, distribution, and oxidation state of each element in the film, in turn depends on its prior treatment. During exposure of AlCr to air when samples are removed from vacuum following deposition, aluminum oxide forms on the surface and protects the chromium from oxidation. This is supported by both XAS data[5] and XPS data (curve a in Fig. 15), which show that Cr is not oxidized in as-deposited samples. Cr has

also been found to remain unoxidized during immersion of AlCr alloys in borate solution at open circuit (curve a in Fig. 1 and top curve in Fig. 4). Curve d in Fig. 15 shows that slow scanning of the potential from open circuit to 0 V causes dissolution of aluminum and oxidation of some of the Cr in the alloy to Cr(III). The progressive slow stepping performed in the XAS experiments likely results in the same behavior. The condition of samples just prior to passing through the critical potential of +0.2 V is described by curves a and d in Fig. 15 for samples that are stepped directly to a high potential and samples whose potentials are scanned slowly, respectively. In the first case, Cr is unoxidized and exists in a metallic alloy with Al beneath an aluminum oxide surface film. In the second case, the surface oxide consists of both Al(III) and Cr(III), and the underlying metallic phase is almost entirely Cr in content. There are, therefore, differences in the composition of both the surface oxide and metallic phases for the two conditions. Two possible scenarios, one based on the differences in the surface oxide and one based on differences in the metallic phase, will be presented to describe the behavior of Cr in the AlCr alloys.

One explanation for the comparatively small dissolution upon stepping the potential from open circuit directly to a high potential is the presence of the alumina on the surface at open circuit. It is possible that this oxide protects the alloy. When pure Al is stepped directly to a high potential, it tends to anodize to form a thick oxide film. During direct polarization of the AlCr alloy to a potential above the critical potential, this tendency for anodization results in the simultaneous oxidation of both Al and Cr to form a mixed oxide layer. The presence of the alumina surface film may help prevent dissolution of this mixed oxide during the anodization process. Slow polarization at low potentials results in removal of the alumina oxide layer and the formation of a mixed oxide layer. When this structure is then exposed to potentials above the critical potential for transpassive dissolution, either by continued slow scanning as in curve b of Fig. 15 or by jumping as in curve e of Fig. 15, Cr can dissolve because the Cr-containing oxide is exposed at the surface and not protected by an alumina layer. One problem with this explanation is the behavior described in Fig. 10. After stepping the potential to 2 V, back to −1.5 V, and then increasing the potential slowly through the critical potential, there is no evidence of dissolution of Cr from the mixed oxide despite the expected dissolution of the surface alumina layer during the slow potential increase. However, it is possible that the presence of the thicker mixed oxide on the second cycle may modify the potential distribution across the oxide film, thus reducing the susceptibility of the outer alumina layer to dissolution.

An alternate explanation for the behavior of these AlCr alloys is obtained by focusing on the second difference in the initial condition as described above; the concentration of the underlying metallic layer. Slow scanning at low potentials results in preferential dissolution and oxidation of Al, leading to enrichment of Cr in the underlying metallic layer, as shown in curve d of Fig. 15. When the potential is scanned further, *i.e.*, past the critical potential and into the transpassive potential region, Cr in this layer oxidizes to chromate and dissolves into solution to result in the situation represented by curve b in Fig. 15. The XPS peaks associated with the oxide components are unchanged, while the Cr(0) peak disappears to leave only a mixed Al(III)-Cr(III) oxide. A similar situation develops for a sample that was slowly polarized to 0 V and then stepped to 0.5 V. Having been in essentially the same condition just prior to passing the critical potential, it also exhibits dissolution of Cr to leave a mixed Al-Cr oxide, curve e in Fig. 13. The Cr-rich metallic phase thus behaves like pure Cr upon reaching the critical potential in that it dissolves as chromate. According to this view, Cr is stable once it enters the mixed Al-Cr oxide film, regardless of subsequent polarization treatments, and exhibits different dissolution behavior than pure Cr oxide by being much less susceptible to transpassive dissolution. The Cr ions in this

mixed oxide previously have been found to exhibit different characteristics than Cr ions in other forms.[5,13] For instance, Cr(VI) in a mixed anodic Al-Cr oxide exhibited a reduced signal from the Cr LVV Auger transition, which is of interatomic character, compared to both a pure chromate standard and chromate adsorbed onto an aluminum oxide passive film.[5,13] The change in the Auger signal reflects a change in the electronic structure for Cr(VI) in the anodic film compared to the other forms of Cr(VI). The dissolution behavior described here may also be linked to the altered electronic properties. One distinct feature of the mixed oxide is that the Al 2p peak associated with Al(III) shifts to lower binding energy when the oxide contains Cr as a result of a change in the oxide conductivity, which produces a decrease in the surface charging effect.

In contrast to the behavior during slow scanning, Cr does not dissolve during abrupt stepping of the potential from open circuit to a high value according to this view because the Cr and Al oxidize simultaneously. The Cr thus has a chance to imbed itself in the stable mixed oxide instead of dissolving. Previous XPS data has shown that oxidation to 5 V for 5 min results in a Cr(VI)-containing mixed oxide with Cr:Al concentration that is independent of the initial concentration over a wide range of initial concentration.[5]

One problem with the explanation of behavior based on the composition of the metal layer is that it relies on trans-passive dissolution of the underlying Cr-rich metallic layer despite the presence of the overlying mixed oxide. Such dissolution could take place through defects in the oxide or at local inhomogeneities. As described above, there is some indication that the AlCr layer thins in spots to result in oxidation of Nb that is exposed at the surface. Such sites may also allow dissolution of chromate. However, detailed evidence of such a process is lacking.

The dissolution of Cr from AlCr upon slow anodic polarization thus occurs either because of the loss of the protective alumina surface film at low potentials which exposes Cr in the mixed oxide at the surface or because preferential oxidation of Al leads to an enrichment of Cr in the underlying metallic layer. Either process will lead to the dissolution of Cr as chromate at transpassive potentials. The phenomena studied in this paper may not be as pronounced in thicker alloy films, which would have a larger source of metal atoms that might diminish the effect of Al surface segregation.

Conclusions

Using *in situ* x-ray absorption spectroscopy, the behavior of Cr in AlCr thin films has been found to depend on the sequence of polarization. Slow scanning or incremental stepping of the potential from open circuit through a critical value of +0.2 V(MSE) resulted in dissolution of much of the Cr. Direct stepping of the potential from open circuit to a value above the critical potential resulted in incorporation of Cr into the Al oxide matrix where it was stable and could further oxidize to Cr(VI) without dissolving. XPS analysis determined that slow polarization at low potentials altered the composition of both the surface oxide and metallic phases, replacing the ambient-formed alumina surface film with a mixed Al-Cr oxide layer and enriching Cr in the underlying metal. These changes may be responsible for the dissolution of Cr exhibited during slow potential scanning.

Acknowledgments

A. J. D. and H. S. I were supported under the auspices of the U. S. Department of Energy, Division of Materials Sciences, Office of Basic Energy Science under Contract No. DE-AC02-76CH00016. Measurements were carried out at Beamline XI9A at the National Synchrotron Light Source, Brookhaven National Laboratory. The authors wish to thank Lars Furenlid for assistance with the Beamline and Steve Cramer for the use of the Canberra detector.

IBM Research Division, T. J. Watson Research Center assisted in meeting the publication costs of this article.

REFERENCES

1. J. K. Hawkins, H. S. Isaacs, S. M. Heald, J. Tranquada, G. E. Thompson, and G. C. Wood, *Corros. Sci*, **27**, 391 (1987).
2. S. W M. Chung, J. Robinson, G. E. Thompson, G. C. Wood, and H. S. Isaacs, *Philos. Mag. B*, **63**, 557 (1991).
3. S. W. M. Chung, G. E. Thompson, G. C. Wood, J. Robinson, and K. Shimizu, in *X-Ray Methods in Corrosion and Interfacial Electrochemistry*, A. J. Davenport and J. G. Gordon, Editors, PV 92-1, p. 325, The Electrochemical Society Proceedings Series, Princeton, NJ (1992).
4. J. S. Wainright, M. R. Antonio, and O. J. Murphy, in *ibid.*, p. 315.
5. G. S. Frankel, A. G. Schrott, C. V. Jahnes, M. A. Russak, A. J. Davenport, and H. S. Isaacs, *This Journal*, **139**, 1812 (1992).
6. A. J. Davenport, H. S. Isaacs, G. S. Frankel, A. G. Schrott, C. V. Jahnes, and M. A. Russak, *ibid.*, **138**, 337 (1991).
7. M. Kerkar, J. Robinson, and A. J. Forty, *Faraday Discuss. Chem. Soc*, **89**, 31 (1990).
8. J. Robinson, in *X-Ray Methods in Corrosion and Interfacial Electrochemistry*, A. J. Davenport and J. G. Gordon, Editors, PV 92-1, p. 239, The Electrochemical Society Proceedings Series, Princeton, NJ (1992).
9. J. A. Bardwell, A. J. Davenport, H. S. Isaacs, G. I. Sproule, B. MacDougall, and M. J. Graham, *This Journal*, **139**, 371 (1992), and in *X-Ray Methods in Corrosion and Interfacial Electrochemistry*, *A.* J. Davenport and J. G. Gordon, Editors, PV 92-1, p. 254, The Electrochemical Society Proceedings Series, Princeton, NJ (1992).
10. A. J. Davenport and H. S. Isaacs, Paper 74 in *Corrosion 91*, *NACE*, Cincinnatti, OH, Meeting, March 1991.
11. F W. Kutzler, C. R. Natoli, D. K. Misemer, S. Doniach, and K. O. Hodgson, *J. Chem. Phys.*, **73**, 3274 (1980).
12. M. Pourbaix, *Atlas of Electrochemical Equilibria in Aqueous Solutions*, Pergamon Press, Inc., New York (1966).
13. A. G. Schrott, G. S. Frankel, A. J. Davenport, H. S. Isaacs, C. V Jahnes, and M. A. Russak, *Surf. Sci.*, **250**, 139 (1991).